DHCR24 inhibition upregulates desmosterol without promoting regression of atherosclerotic plaques in APOE*3-Leiden.CETP mice

Miao, J.; Zijlstra, L.F.; Heijink, M.; Sidorov, I.; Vaart, J.I. van der; Müller, C.; ... ; Kooijman, S.

Steroids 235–236 (2026) 109830

Contents lists available at ScienceDirect

Steroids

journal homepage: www.elsevier.com/locate/steroids

DHCR24 inhibition upregulates desmosterol without promoting regression of atherosclerotic plaques in APOE*3-Leiden.CETP mice

Jing Miao [a,b,1], Lobke F. Zijlstra [c,d,e,1], Marieke Heijink [b], Iulia Sidorov [b], Jamie I. van der Vaart [a], Christoph Müller [f], Franz Bracher [f], Menno P.J. de Winther [c,d,e], Martin Giera [b], Annette E. Neele [c,d,e], Patrick C.N. Rensen [a], Sander Kooijman [a,*]

[a] Department of Medicine, Division of Endocrinology, and Einthoven Laboratory for Experimental Vascular Medicine, Leiden University Medical Center, Leiden, the Netherlands
[b] Center for Proteomics and Metabolomics, Leiden University Medical Center, Leiden, the Netherlands
[c] Amsterdam UMC, location University of Amsterdam, Department of Medical Biochemistry, Amsterdam, the Netherlands
[d] Amsterdam Cardiovascular Sciences, Atherosclerosis & Ischemic Syndromes, Amsterdam, the Netherlands
[e] Amsterdam Institute for Immunology and Infectious disease, Amsterdam, the Netherlands
[f] Department of Pharmacy, Center for Drug Research, Ludwig Maximilians University Munich, Munich, Germany

ARTICLE INFO

Keywords:
Liver X receptor
Desmosterol
Atherosclerosis regression
Δ24-dehydrocholesterol reductase
Peritoneal macrophages

ABSTRACT

Background and Aims: Inhibition of Δ24-dehydrocholesterol reductase (DHCR24) leads to accumulation of the cholesterol biosynthesis intermediate desmosterol, which is the endogenous ligand for liver X receptors (LXRs). Activation of LXRs is considered to be atheroprotective as it suppresses inflammation and stimulates cholesterol efflux in macrophages *via* upregulation of ATP-binding cassette transporters A1 and G1. In the current study we aimed to investigate the effect of the selective DHCR24 inhibitor SH42 on regression of atherosclerotic plaques in APOE*3-Leiden.CETP mice, a well-established model for human-like lipid metabolism.

Methods: Mice were fed a Western-type diet (16% fat, 0.15% cholesterol) for 20 weeks to promote plaque development. Subsequently, treatment was started with vehicle or SH42 for 8 weeks while the animals were kept on a regular chow diet.

Results: Treatment with SH42 significantly upregulated desmosterol levels in liver and plasma, and led to a small reduction in plasma triglyceride, nonHDL-cholesterol and HDL-cholesterol levels on top of the lipid-lowering effect caused by the dietary switch. While SH42 treatment did not affect immune cell numbers in blood, bone marrow, or spleen, SH42 strongly reduced the number of macrophages found in the peritoneum after thioglycolate injection.

Conclusions: While the dietary switch halted atherosclerotic lesion progression, SH42 treatment did not accelerate atherosclerotic lesion regression further.

1. Introduction

Atherosclerosis refers to build up of lipid-rich plaques in and on arteries, and is a common disease that hampers blood flow and comes with the risk of heart attack or stroke when plaques rupture. Dyslipidemia (*i.e.* high triglycerides, high LDL-cholesterol, and low HDL-cholesterol) and inflammation are major risk factors as they drive atherosclerotic plaque progression. Currently available treatments in primary and secondary prevention of atherosclerotic cardiovascular diseases are primarily directed at preventing progression through lowering circulating cholesterol levels (*e.g.* statins and inhibitors of NPC1L1 and PCSK9). Very recently low-dose colchicine (0.5 mg daily) was approved as the first anti-inflammatory therapy to be used on top of statins. [1] A therapeutic approach that not only halts lesion development but actually promotes regression of atherosclerotic lesions is highly desirable.

Targeting liver X receptors (LXRs) has been identified as an approach

* Corresponding author at: Department of Medicine, Division of Endocrinology, Leiden University Medical Center, P.O. Box 9600, 2300 RC, Leiden, the Netherlands.
E-mail address: s.kooijman@lumc.nl (S. Kooijman).
[1] Authors contributed equally.

https://doi.org/10.1016/j.steroids.2026.109830
Received 21 January 2026; Received in revised form 14 July 2026; Accepted 14 July 2026
Available online 15 July 2026

to facilitate lesion regression. [2–4] LXR activity interferes with atherosclerosis *via* regulation of gene expression of at least two relevant signaling pathways. Firstly, LXR promotes reverse cholesterol transport through upregulation of cholesterol exporters ATP-binding cassette transporters A1 (ABCA1) and G1 (ABCG1). Secondly, LXR has a general inhibitory effect on proinflammatory gene expression, by recruiting co-repressors to NF-κB. [5] Indeed, treatment of mice with LXR agonists has been shown to protect against atherosclerosis development [6,7] and, most importantly, promote regression of existing atherosclerotic plaques. [8,9] A major disadvantage of the use of synthetic LXR agonists, however, is that they cause hepatic steatosis and hyperlipidemia *via* activating sterol regulatory element-binding protein 1c (SREBP-1c), fatty acid synthase (FAS), and stearoyl-CoA desaturase 1 (SCD1) in hepatocytes. [10,11] We thus need a strategy to specifically activate LXR in macrophages. In fact, the liver-selective LXR inverse agonist SR9238 is currently being evaluated as a treatment for metabolic dysfunction-associated steatotic liver disease (MASLD). [12,13]

Intriguingly, desmosterol was identified as the endogenous ligand for LXR in macrophages but not hepatocytes, [14,15] and we previously demonstrated that inhibition of Δ24-dehydrocholesterol reductase (DHCR24), the enzyme catalyzing the conversion of desmosterol into cholesterol, leads to accumulation of desmosterol in livers and blood of mice. [16,17] Subsequent experiments with the steroidal inhibitor of DHCR24, namely SH42, provided further evidence for a role of desmosterol in stimulating cholesterol efflux from macrophages *in vitro* and inflammation resolution *in vivo*. [18,19] In contrast to our expectations, however, we did not observe protection from atherosclerosis development upon treatment of APOE*3-Leiden.CETP mice or *LDLr*$^{-/-}$ mice with SH42. [20] A plausible explanation for the lack of atheroprotective effects of DHCR24 inhibition relates to the model used to investigate atherosclerosis. This model relies on a high cholesterol-diet, potentially causing severe, perhaps even unphysiological hypercholesterolemia and lesion progression. [21] Therefore, in the current study we evaluated the potential of SH42 in APOE*3-Leiden.CETP mice under regressive, cholesterol-free diet, conditions.

2. Materials and methods

2.1. Animals and treatments

The animal experiments have been performed in compliance with the guidelines of the Dutch Act on Animal Experimentation and EU Directive 2010/63/EU, and received prior approval by the Animal Welfare Body Leiden and Central Authority for Scientific Procedures on Animals (CCD; license number AVD11600202010187).

APOE*3-Leiden.CETP mice (C57BL/6 J background) were generated by crossbreeding hemizygous APOE*3-Leiden transgenic mice with homozygous human cholesteryl ester transfer protein (CETP) transgenic mice as previously described. [22] All mice were housed under a standard 12-h light-dark cycle at 22 °C with *ad libitum* access to water and food, unless indicated otherwise. At 8–12 weeks of age, female APOE*3-Leiden.CETP mice were switched from a regular chow diet to a Western-type diet (WTD; containing 16% fat and 0.15% cholesterol; Ssniff, Germany) to induce hyperlipidemia and promote atherosclerotic lesion development. After 20 weeks of WTD feeding, mice were divided into three blocks (n = 19 per block) that were balanced for body weight, body composition, and 4 h-fasted plasma triglyceride (TG) and total cholesterol (TC) levels using RandoMice v1.0.9. [23] These blocks were randomly assigned to the experimental groups. A first 'baseline' group of mice was killed without further intervention. The two remaining groups were switched from the WTD back to a regular chow diet, and mice of those groups were three times per week (*i.e.*, Monday, Wednesday, and Friday) intraperitoneally injected with either vehicle (7.5 μL ethanol and 7.5 μL Cremophor EL added to 135 μL saline) or SH42 (0.5 mg in 150 μL vehicle) for another 8 weeks. At the start of week 4 and 8 of treatment, body weight, and body composition were determined, and 4 h-fasted blood was collected for measurement of plasma lipids and blood leukocyte subsets with flow cytometry. Four days before the end of the experiment, a subset of mice received an intraperitoneal injection with thioglycolate medium (3% in sterile PBS) to induce sterile inflammation. All animals were killed after 8 weeks of treatment to collect hearts for assessment of atherosclerotic lesions. The mice that had received the thioglycolate medium (n = 5 per group) were additionally used to isolate immune cells after peritoneal lavage. The remaining mice (n = 14 per group) were used to collect additional blood *via* heart puncture and tissues including spleen and bone marrow for flow cytometry, and liver for histological assessment and molecular analyses.

2.2. Body weight and composition

Body weight was determined on a 2-decimal weighing scale. Body composition (*i.e.* lean mass and fat mass) was assessed using an EchoMRI-100 analyzer (EchoMRI, USA).

2.3. Plasma lipids

Blood collected in EDTA-coated tubes was centrifuged at 2100 rcf for 10 min to obtain plasma, in which TG and TC levels were measured using enzymatic kits (Roche Diagnostics, Germany). HDL-C was quantified following precipitation of apolipoprotein B (ApoB)-containing lipoproteins. Briefly, plasma was mixed with 20% polyethylene glycol (PEG)6000 (Sigma-Aldrich, USA) prepared in 200 mM glycine-buffered saline (pH 10, 1:2, *v*/v), followed by centrifugation at 6000 rpm for 30 min. HDL-C concentrations were determined by measuring TC in the obtained supernatant as described above. Plasma non-HDL cholesterol (non-HDL-C) was calculated by subtracting HDL-C from TC levels. [24]

2.4. Liver lipids

Hepatic lipids were isolated from frozen liver samples as previously reported. [25] Briefly, approximately 50 mg of liver tissue was homogenized in CH_3OH (10 μL/mg tissue). An aliquot of the homogenate (45 μL) was mixed with 1800 μL CH_3OH:$CHCl_3$ (1:3, *v*/v) and centrifuged at 20,000 *g* for 15 min at room temperature. The resulting organic phase was collected and dried under a gentle stream of N_2, and resuspended in 100 μL of 2% Triton X-100 in $CHCl_3$. Following a second drying step under N_2, the samples were reconstituted in 100 μL of H_2O for biochemical analyses. TG and cholesterol (Roche Diagnostics, Germany) and phospholipids (Instruchemie, The Netherlands) were measured *via* enzymatic kits. Protein concentrations were measured using a BCA Protein assay kit (ThermoFisher, USA). Hepatic lipids were expressed as nmol per mg protein. All samples were measured in duplicate with an acceptable coefficient of variation below 15%.

2.5. Liver gene expression

Total RNA from snap-frozen liver samples was extracted by Tripure RNA isolation reagent (Sigma-Aldrich, USA) based on the manufacturer's instructions. Moloney Murine Leukemia Virus Reverse Transcriptase (Promega, USA) was added to initiate reverse transcription from 1 μg RNA into complementary DNA. Quantitative real-time PCR was performed using SYBR green (Promega, USA) and fluorescence signal was detected by a qPCR CFX96 Bio-Rad machine. mRNA expression levels were normalized to *Gapdh* mRNA level and expressed as fold change compared with the baseline or vehicle group using the $2^{-\Delta\Delta Ct}$ method. Primer sequences are listed in **Table S1**.

2.6. Peritoneal cell cultures

Peritoneal cells were collected from the animals that received an intraperitoneal injection with thioglycolate (3% in sterile PBS). To this end, the peritoneal cavity was flushed with 10 mL of ice-cold phosphate-

buffered saline (PBS). Red blood cells were removed by 1 min incubation with red blood cell lysis buffer (Invitrogen, USA) and peritoneal cells were subsequently cultured in Roswell Park Memorial Institute (RPMI) 1640 Medium containing 25 mM HEPES and supplemented with 2 mM L-glutamine (Gibco, USA), 10% fetal calf serum (Gibco, USA), penicillin (100 U/mL, Gibco, USA), and streptomycin (100 mg/mL, Gibco, USA) in a density of 1*10^6 cells/ml in either 24 wells (500 µL) or 96 wells (150 µL) tissue culture plates (Greiner Bio-One, Netherlands). After a three-hour adherence period the cells were either washed and stained with Oil Red O or stimulated with the following cytokines: 24 h with IL-4 (50 ng/mL, Peprotech, USA) and 6 h with lipopolysaccharide (LPS; 10 ng/mL, Sigma, O55:B5, USA) for RNA analysis, or 24 h with LPS (10 ng/mL) for protein analysis, or left unstimulated.

2.7. Peritoneal cell gene expression

Total RNA was isolated from peritoneal cells using the GeneJET RNA Purification Kit (Thermo Fisher, USA) following the manufacturer's protocol. Obtained RNA was reverse transcribed into cDNA with use of the High-Capacity cDNA Reverse Transcription Kit (Applied Biosystems, USA). Real-time quantitative PCR (qPCR) was conducted using 4 ng of cDNA and Fast SYBR™ (Applied Biosystems, USA) on a QuantStudio 5 real time PCR system (Applied Biosystems, USA). Relative gene expression levels were calculated by normalizing them to the averaged expression level of CYCLO and ARBP. Primer sequences are listed in **Table S2**.

2.8. Oil red O staining

To visualize foam cell formation, peritoneal cells were plated on the 8-well Nunc Lab-Tek Chamber Slide System (Thermo Scientific, USA), and lipids were stained with an Oil red O staining (0.3% in 60% isopropanol, Sigma-Aldrich, USA). Pictures were made with a Leica DM6B.

2.9. Flow cytometry

Blood was obtained *via* a tail cut and collected into EDTA-coated tubes. A whole blood analysis was conducted using a Scil Vet abc plus+ veterinary hematology analyzer with 10 µL of blood to assess white blood cells, red blood cells, and platelets. Subsequently, the remaining blood was centrifuged at 2100 rcf for 10 min at 4 °C to separate the blood cells from the plasma. The spleen was homogenized and filtered through a 70 µm cell strainer (Corning, USA) and bone marrow was flushed from femurs using PBS. Next, blood cells, spleen, and bone marrow were subjected to red blood cell lysis (150 mM ammonium chloride and 10 mM sodium bicarbonate, 5 mM EDTA, pH 7.4) until cell pellets were white. Peritoneal cells were washed with PBS and incubated with TrypleE (Gibco, USA) for 15 min at 37 °C and hereafter lifted and neutralized using FACS buffer (PBS, 0.5% BSA, 5 mM EDTA). All cells were blocked and stained in FACS buffer containing fluorescently labeled antibodies (**Table S3–10**) and Fc receptor block (1:1000 Biolegend, 101330, USA), for 30 min at 4 °C. Before analysis, 7-AAD (1:1000 Thermo Fisher Scientific, #A1310, USA) or DAPI (1:10,000 Thermo Fisher Scientific, D21490, USA) was added to exclude dead cells. To visualize lipid uptake by flow cytometry, peritoneal cells were stained with LipidTOX (1:200 Invitrogen, H34476, USA) to visualize lipid content in combination with LIVE/DEAD Fixable Near IR (780) (1:1000 Invitrogen, L34994, USA) to exclude dead cells. Stained cells were analyzed on a LSR Fortessa Cell Analyzer (BD Biosciences, USA), Symphony A1 Cell Analyzer (BD Bioscience, USA), or Cytoflex S (Beckman Coulter, USA) and analyzed using FlowJo version 10 (BD Biosciences, USA).

2.10. Desmosterol measurement

Tail vein plasma and a fixed weight (50–100 mg) liver piece were isolated and total desmosterol levels were quantified. Liver tissue was homogenized in H_2O to a final concentration of 0.2 mg liver/µL homogenate with a Bullet Blender Gold (Next Advance, USA) for 5 min at 4 °C using stainless steel beads (0.9–2.0 mm blend; Next Advance, USA). Homogenized liver (12.5 µL) or plasma (10 µL) samples were further saponified at 70 °C for 1 h using 1 M sodium hydroxide in 80% ethanol containing desmosterol-*d6* (Avanti Research, USA). Samples were further processed by solid phase extraction (SPE) on Strata™-X 33 µm polymeric reversed-phase cartridges (Phenomenex, USA) using methyl formate (Sigma-Aldrich, Germany) as elution solvent. The extracts were dried and desmosterol was derivatized into its trimetylsilyl ether derivative before gas chromatography–mass spectrometry (GC–MS) analysis. The GC was equipped with a VF-5 ms column (Agilent, USA). The MS was equipped with an electron ionization source and operated in single ion monitoring mode. As quantifier ions for desmosterol and desmosterol-*d6* *m/z* 327.2 and 333.3 were used, respectively. The full step-by-step protocol containing all the materials, method details and instrumental settings are described elsewhere. [26]

2.11. Atherosclerotic lesion quantification

Formaldehyde-fixated, paraffin embedded hearts were cross-sectioned at the level of the aortic root with 50 µm intervals. Sections were stained with hematoxylin-phloxine-saffron (HPS) for quantification of atherosclerotic lesion size. Lesion severity was scored subjectively after blinded according to the guideline of the American Heart Association adapted for mice as we previously reported (mild lesion: type I-III, plaque with infiltrated foam cells and probably with a fibrotic cap; severe lesion: type IV-V, media fibrosis and the presence of cholesterol clefs/mineralization/necrosis). [27] Smooth muscle cells within the media were stained using an anti-a-actin antibody (M0851, Dako, Denmark) and a secondary antibody EnVision System-HRP Labeled Polymer (Dako, Denmark). Macrophages area were stained with a rat monoclonal anti-Mac-3 antibody (BD Pharmingen, USA). 0.1% Sirius Red (Sigma-Aldrich, USA) was used to quantify collagen distribution. Stability index was calculated as (smooth muscle cells area % + collagen area %) / macrophage area % within the lesion area. All specific stained areas were quantified using Image J software v1.52a.

2.12. Statistical analysis

GraphPad Prism Software, v9.3 was applied for all data assessment. Differences between vehicle and SH42 groups were compared using unpaired two-tailed Student's *t*-tests, Mann Whitney *U* test or Two-way ANOVA. One-way ANOVA with Tukey post-hoc analysis was used to compare the different parameters among baseline, vehicle and SH42 treatments. Statistical outliers within the group were excluded by Grubb's test. Data are presented as mean ± SEM. *P* values less than 0.05 were considered statistically significant; P values greater than 0.05 and less than 0.10 were considered as a trend.

3. Results

3.1. SH42 increases desmosterol and lowers plasma lipids levels in a mouse model of atherosclerosis regression

APOE*3-Leiden.CETP mice were fed a cholesterol-containing WTD to promote atherosclerotic lesion development. After 20 weeks, a group of animals was killed to establish the baseline atherosclerotic lesion size and composition. The remaining animals were switched to a regular chow diet to stop lesion progression, and facilitate lesion regression. During this 8 week period, mice were treated with either vehicle or the DHCR24 inhibitor SH42 (Fig. 1A). We first confirmed accumulation of desmosterol in liver (Fig. 1B) and plasma (Fig. 1C) after 8 weeks of treatment with SH42. Interesting enough, in the absence of excessive dietary cholesterol, treatment with SH42 that inhibits the enzyme

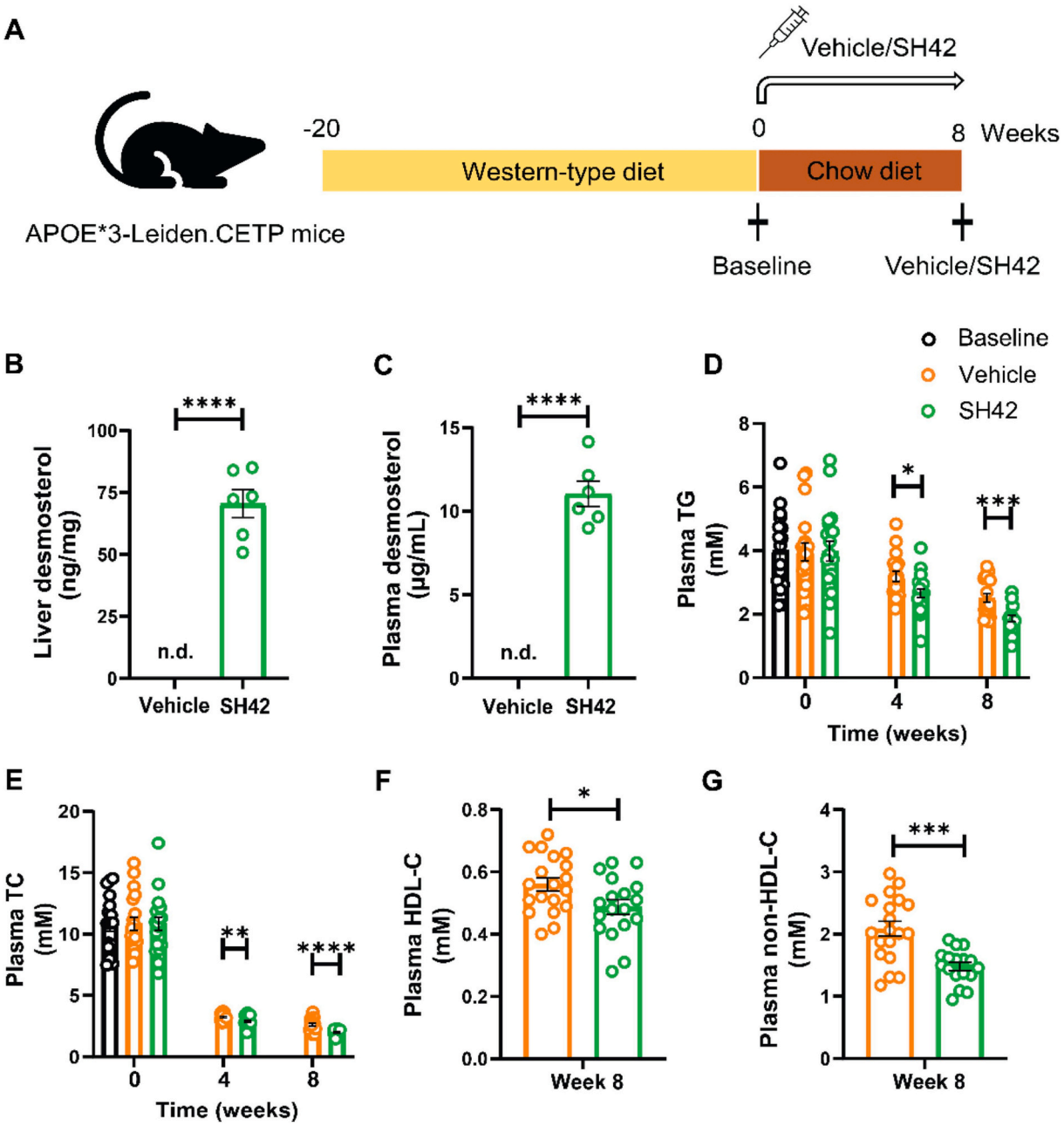

Fig. 1. DHCR24 inhibition increases desmosterol levels in the liver and plasma, while decreases plasma lipid levels in APOE*3-Leiden.CETP mice. APOE*3-Leiden.CETP mice received a Western-type diet containing 16% fat and 0.15% cholesterol for 20 weeks (baseline), before they were switched to a cholesterol-free chow diet while receiving intraperitoneal injections with either SH42 (0.5 mg/mouse) or vehicle 3 times per week for 8 weeks (**A**). Liver (**B**) and plasma (**C**) desmosterol concentrations were measured by GC–MS. Plasma triglycerides (TG) (**D**), total cholesterol (TC) (**E**), high-density lipoprotein-cholesterol (HDL—C) (**F**) and non-high density lipoprotein-cholesterol (non-HDL-C) (G) were measured at week 4 or week 8. n.d., non-detectable. Data are presented as mean ± SEM. B-C: 6 mice per group; D-G: $n = 17$–19 mice per group. B-G: data were analyzed by two-tailed Mann Whitney U test. *$P < 0.05$, **$P < 0.01$, ***$P < 0.001$, ****$P < 0.0001$.

facilitating the final step in *de novo* cholesterol synthesis, also led to a reduction in plasma TG (−26%; Fig. 1D) and TC (−25%; Fig. 1E) on top of the lipid-lowering effects of the switch from WTD to regular chow diet. The reduction in circulating TC levels in SH42 compared to vehicle treated mice was explained by lower HDL-C (−13%; Fig. 1F) and non-HDL-C (−29%; Fig. 1G) levels. Body weight (**Fig. S1A**), fat mass (**Fig. S1B**) and lean mass (**Fig. S1C**) were not different between the groups at baseline, and the switch from WTD to regular chow led to a reduction in fat mass similarly in vehicle and SH42 treated mice. Consistent with this observation we observed equally lowered white adipose tissue weights in vehicle and SH42 treated mice compared to animals of the baseline group (**Fig. S1D**). Subcutaneous brown adipose tissue (sBAT) and skeletal muscle (**Fig. S1D**) weights were slightly elevated in SH42 compared to vehicle treated mice at the end of the study.

3.2. *SH42 does not promote hepatic steatosis or inflammation in APOE*3-Leiden.CETP mice*

As synthetic LXR agonists are known to promote hepatic steatosis and inflammation as a side effect, we next performed a histological assessment of the liver. In line with previous reports, [19,20] we found

no evidence for SH42 to cause such effects (Fig. 2A). The switch from WTD to regular chow led to a significant reduction in lipid area hepatic TG and TC levels, although to a lesser extent in SH42 compared to vehicle treated mice (Fig. 2B). The dietary switch caused a strong reduction in the hepatic expression of genes involved in *de novo* lipogenesis (*Srebf1c*, *Fasn*, *Acc1*), cholesterol efflux (*Abca1, Abcg1, Abcg5*), and inflammation (*F4/80*, *Tnf-α*, *Il-1b*). However, hepatic gene expression involved in these pathways, in addition to lipolysis (*Hl*, *Atgl*, *Hsl*) and VLDL production (*Apob*, *Mttp*), was not different between vehicle or SH42 treatment (Fig. 2C).

3.3. SH42 attenuates peritoneal macrophage accumulation upon induction of sterile inflammation in APOE*3-Leiden.CETP mice

To investigate the effect of SH42 on immune cell function under a regressive, cholesterol-free dietary condition, we continued with studying the accumulation of peritoneal monocytes and macrophages after induction of sterile inflammation with thioglycolate. Most strikingly, four days after induction only few peritoneal cells could be harvested from SH42 mice compared to vehicle treated mice (Fig. 3A). After subsequent cell culture, 41% were classified as macrophages (*i.e.* CD11b + F4/80+) compared to 79% in the vehicle treated mice (Fig. 3B-C). This was further supported by decreased mRNA expression of macrophage markers CD68 and F4/80 (Fig. 3D). Together these data clearly show a decrease of macrophages in the peritoneum of SH42 treated mice. Next, to better explain the peritoneal inflammatory status, anti-inflammatory surface markers CD206 and CD301 were measured with no difference found between vehicle and SH42 after IL-4 activation (Fig. 3E). Finally, we quantified the lipid content of peritoneal macrophages by LipidTox and Oil red O staining, and interestingly we found a dramatic reduction of foam cells after SH42 treatment (Fig. 3F-G).

3.4. SH42 does not affect immune cell subsets in blood, spleen or bone marrow in APOE*3-Leiden.CETP mice

We next examined immune cell subsets in blood, spleen and bone marrow using flow cytometry. After 8 weeks of treatment, we found no differences between vehicle and SH42 treated mice with respect to the number or composition of whole blood cells (Fig. 4A), circulating myeloid cells (Fig. 4B) or lymphoid cells (Fig. 4C), nor was there a

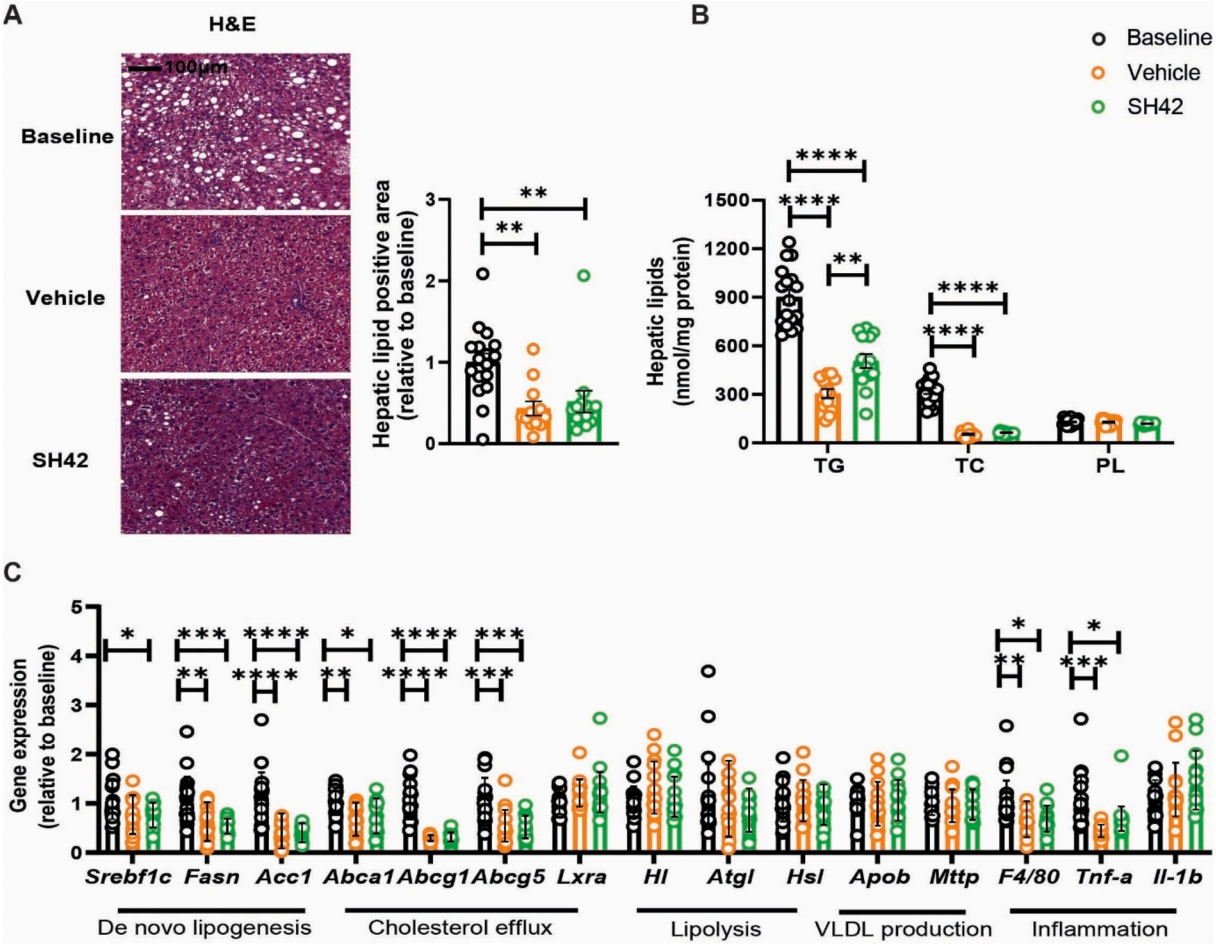

Fig. 2. DHCR24 inhibition does not promote hepatic steatosis or inflammation in APOE*3-Leiden.CETP mice. APOE*3-Leiden.CETP mice received a Western-type diet containing 16% fat and 0.15% cholesterol for 20 weeks (baseline), before they were switched to a cholesterol-free chow diet while receiving intraperitoneal injections with either SH42 (0.5 mg/mouse) or vehicle 3 times per week for 8 weeks. Hematoxylin and eosin (H&E) staining was performed to quantify lipid area in liver (**A**) and triglycerides (TG), total cholesterol (TC) and phospholipids (PL) levels in liver were enzymatically determined (**B**). Relative mRNA expression of hepatic genes related to lipid synthesis and catabolism, transport and inflammation (**C**). *Srebf1c*, sterol regulatory element-binding factor 1c; *Fasn*, fatty acid synthase; *Acc1*, acetyl coenzyme A carboxylase 1; *Abca1*, ATP binding cassette subfamily A member 1; *Abcg1*, ATP binding cassette subfamily G member 1; *Abcg5*, ATP binding cassette subfamily G member 5; *Lxrα*, liver X receptor α; *Hl*, hepatic lipase; *Atgl*, adipose triglyceride lipase; *Hsl*, hormone-sensitive lipase; *Apob*, apolipoprotein B; *Mttp*, microsomal triglyceride transfer protein; *Tnf-α*, tumor necrosis factor α; *Il-1b*, interleukin-1b; *F4/80*, EGF module-containing mucin-like receptor. Data are presented as mean ± SEM. A-C: $n = 13$–17 mice per group. A-C: data were analyzed by one-way ANOVA with Tukey post-hoc analysis. $^{*}P < 0.05$, $^{**}P < 0.01$, $^{***}P < 0.001$, $^{****}P < 0.0001$.

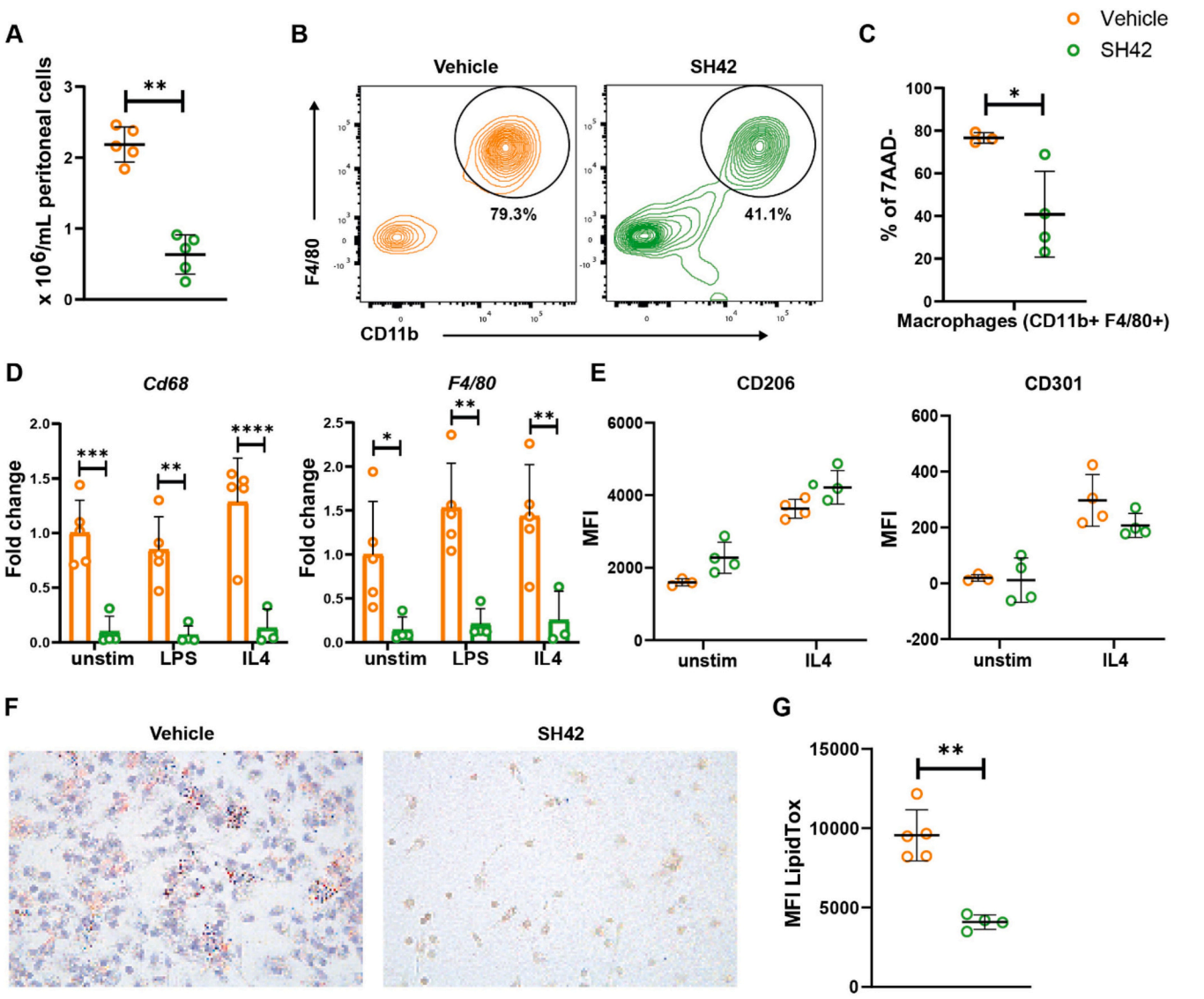

Fig. 3. DHCR24 inhibition attenuates peritoneal macrophage accumulation upon induction of a sterile inflammation in APOE*3-Leiden.CETP mice. APOE*3-Leiden.CETP mice received a Western-type diet containing 16% fat and 0.15% cholesterol for 20 weeks (baseline), before they were switched to a cholesterol-free chow diet while receiving intraperitoneal injections with either SH42 (0.5 mg/mouse) or vehicle 3 times per week for 8 weeks. Four days before the end of the experiment, a subset of mice ($n = 5$ per group) received an intraperitoneal injection with thioglycolate medium to induce sterile inflammation. Total peritoneal cell count (**A**) and macrophage count (**B**—**C**, $CD11b^+$ $F4/80^+$) based on flow cytometry. mRNA expression level of CD68 and F4/80 as determined by qPCR (D). Quantified surface expression values (MFI: Median Fluorescent Intensity) of CD206 and CD301 on macrophages ($CD11b^+$, $F4/80^+$) (E). Oil red O staining (F) and LipidTox staining (G) of *in vitro* differentiated foam cells. *F4/80*, EGF module-containing mucin-like receptor; *Cd68*, cluster of differentiation 68; CD301, cluster of differentiation 301; CD206, cluster of differentiation 206. Data are presented as mean ± SEM. A-G: $n = 3$–5 mice per group. A-C,G: Data were analyzed by unpaired two-tailed Student's *t*-test; D-E: data were analyzed by two-way ANOVA with Šídák's multiple comparisons test. $^*P < 0.05$, $^{**}P < 0.01$, $^{***}P < 0.001$, $^{****}P < 0.0001$. (For interpretation of the references to colour in this figure legend, the reader is referred to the web version of this article.)

change in classical $Ly6C^{high}$ or non-classical $Ly6C^{low}$ monocytes (Fig. 4D). Likewise, splenic myeloid -, B cell - and T cell subset compositions were comparable between the treatment groups, as were the compositions of the bone marrow progenitors and mature bone marrow cells (Fig. 4E-I). Overall, this shows that treatment of mice with SH42 does not affect immune cell proliferation nor change immune cell composition in the blood, spleen, and bone marrow of APOE*3-Leiden. CETP mice during regression induced by regular chow diet.

3.5. SH42 does not accelerate atherosclerotic lesion reversal in APOE*3-Leiden.CETP mice

HPS staining was performed to quantify atherosclerotic lesion size in the aortic root (Fig. 5A-C) and plaque severity (type I-IV; Fig. 5D). As expected, switching mice from WTD to a regular chow diet halted atherosclerotic lesion progression. However, in contrast to our expectations, SH42 administration did not result in lesion regression (Fig. 5A-D). Next, we studied lesion composition (*i.e.* relative contents of smooth muscle cells, macrophages and collagen), which was altered by the switch from WTD to regular chow diet. Compared to baseline, both treatments reduced the macrophage content of the plaques while increasing collagen and smooth muscle content (Fig. 5E-H), resulting in an increased stability index of the plaques (Fig. 5I). Nonetheless, no difference in atherosclerotic plaque composition was observed between vehicle and SH42 treated mice. Together these data show that SH42 does not promote atherosclerotic lesion regression in APOE*3-Leiden. CETP mice.

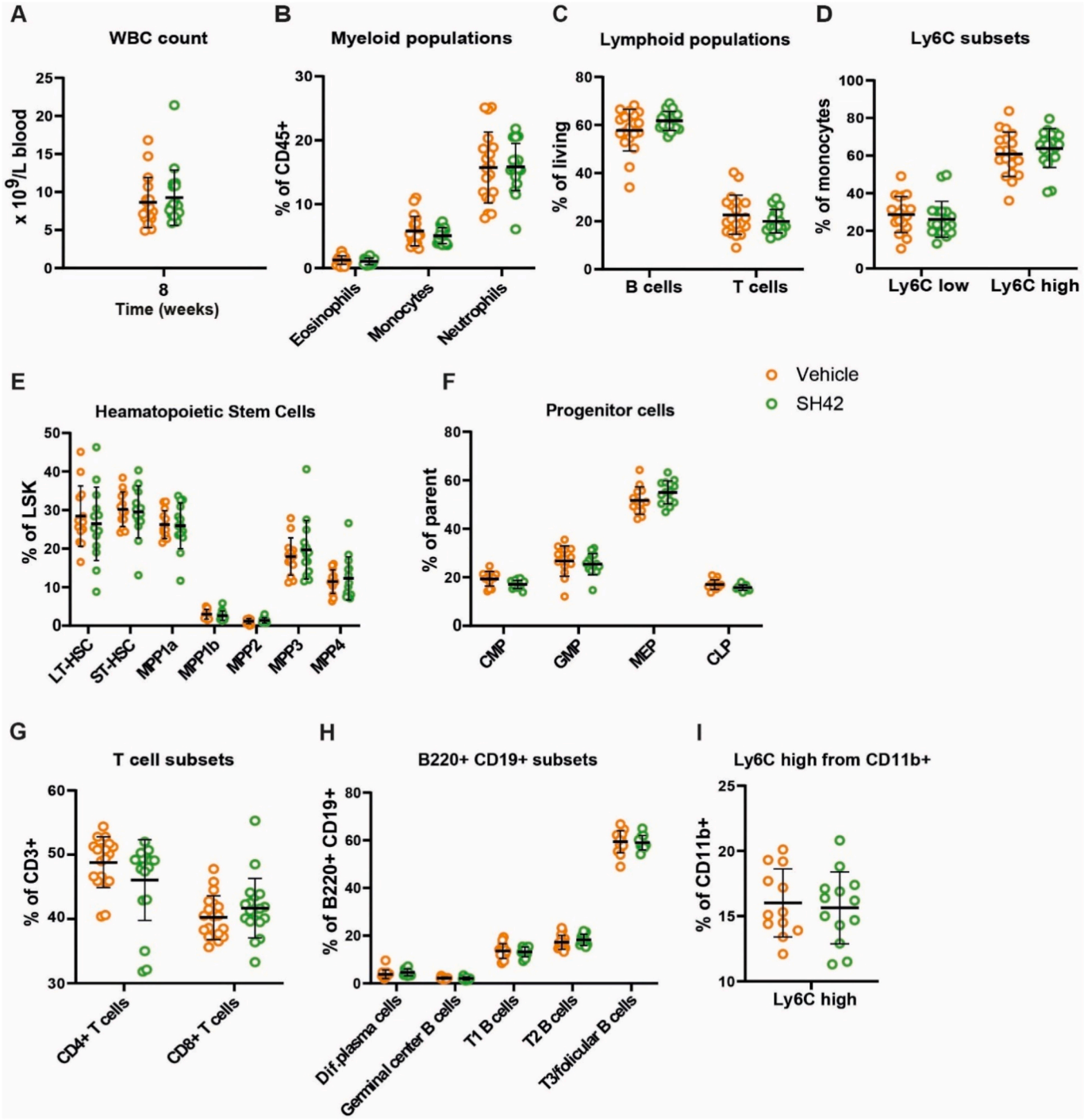

Fig. 4. DHCR24 inhibition does not affect immune cell subsets in blood, spleen or bone marrow in APOE*3-Leiden.CETP mice. APOE*3-Leiden.CETP mice received a Western-type diet containing 16% fat and 0.15% cholesterol for 20 weeks (baseline), before they were switched to a cholesterol-free chow diet while receiving intraperitoneal injections with either SH42 (0.5 mg/mouse) or vehicle 3 times per week for 8 weeks. Total white blood cells (WBC) (A) counts and the percentages of blood myeloid populations (B), lymphoid populations (C), Ly6C^{high} or Ly6C^{low} expressed monocytes (D) based on flow cytometry. Heamatopoietic stem cells (E) and diverse progenitor cells (F) in bone marrow; CD3^{+} T cell (G), B220^{+} CD19^{+} B cells (H), and Ly6C^{high} CD11b^{+} cells (I) in spleen measured by flow cytometry. LSK, Lineage-negative, Sca-1-positive, c-Kit-positive; CMP, common myeloid progenitors; GMP, granulocyte-monocyte progenitor; MEP, megakaryocyte-erythrocyte progenitor; CLP, common lymphoid progenitors. Data are shown as mean ± SEM. A-I: $n = 12$–19 mice per group. A-H: data were analyzed by two-way ANOVA with Šídák's multiple comparisons test; I: data were analyzed by unpaired two-tailed Student's t-test. *$P < 0.05$, **$P < 0.01$, ***$P < 0.001$, ****P < 0.0001.

4. Discussion

Anti-inflammatory lipid mediators hold promise in the treatment of cardiometabolic diseases. Desmosterol is an effective endogenous LXR ligand, which promotes excretion of cholesterol and suppresses inflammation in macrophages, but in contrast to synthetic LXR agonists does not lead to hyperlipidemia or hepatic steatosis. [15,28–31] Here we evaluated whether inhibition of DHCR24 as the enzyme facilitating the conversion of desmosterol into cholesterol, promotes atherosclerosis regression in APOE*3-Leiden.CETP mice. Whilst we found strongly elevated desmosterol concentrations in liver and plasma upon treatment with the selective small molecule DHCR24 inhibitor SH42, accompanied

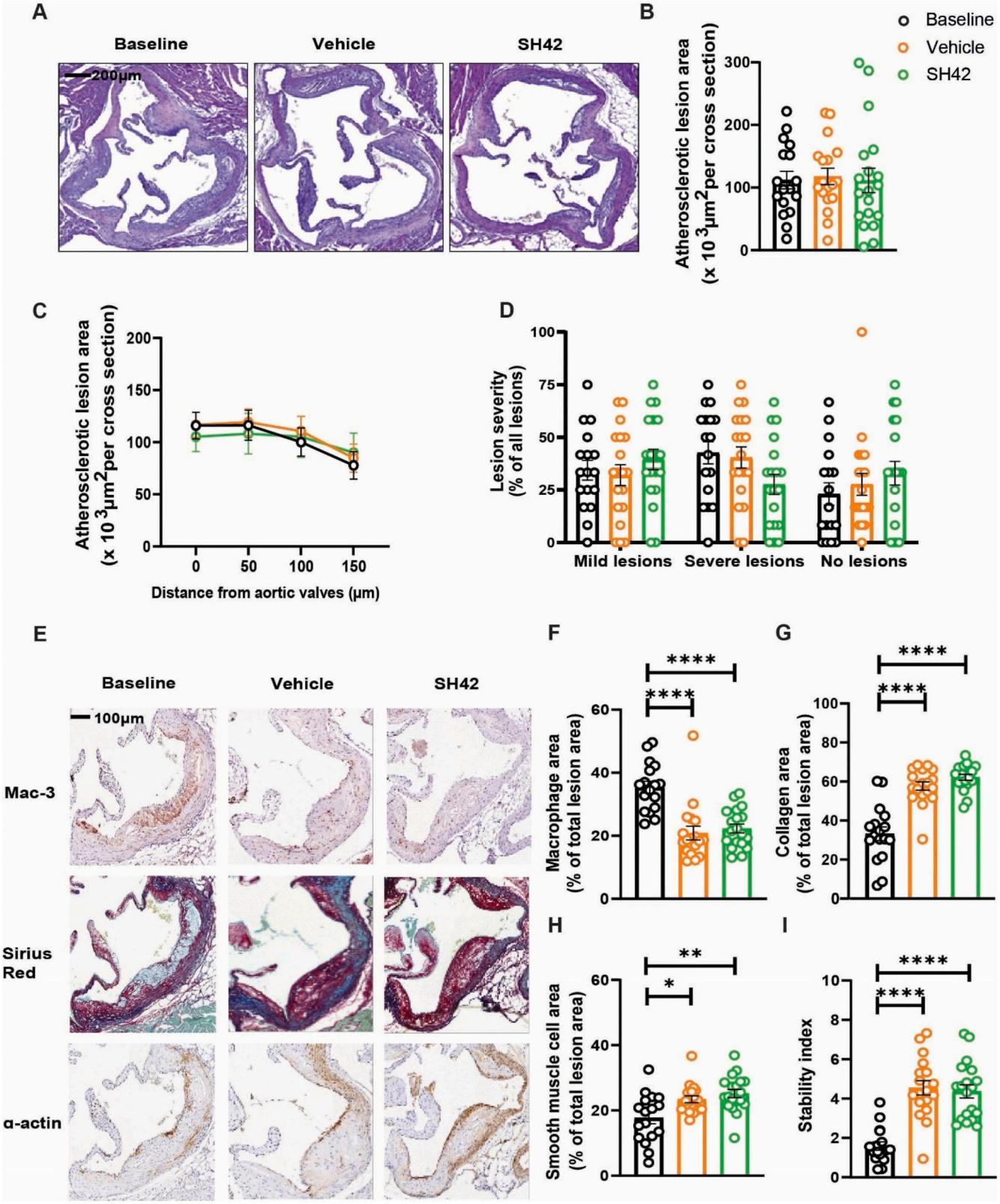

Fig. 5. DHCR24 inhibition does not accelerate the atherosclerotic lesion reversal in APOE*3-Leiden.CETP mice. APOE*3-Leiden.CETP mice received a Western-type diet containing 16% fat and 0.15% cholesterol for 20 weeks (baseline), before they were switched to a cholesterol-free chow diet while receiving intraperitoneal injections with either SH42 (0.5 mg/mouse) or vehicle 3 times per week for 8 weeks. Hearts were isolated and the aortic root valve areas were stained with hematoxylin-phloxine-saffron (HPS), and representative pictures are shown (A). The average atherosclerotic lesion area (B), lesion area at 50 µm intervals from the aortic valves (C), and lesion severity (D). Plaque composition based on MAC-3, Sirius red and α-actin to respectively assess macrophage (F), collagen (G) and smooth muscle cell (H) content. Plaque stability index (*i.e.*, area of smooth muscle cells and collagen divided by the area of macrophages) (I). Data are presented as mean ± SEM. $n = 17$–19 mice per group. Data were analyzed by one-way ANOVA with Tukey post-hoc analysis. *$P < 0.05$, **$P < 0.01$, ***$P < 0.001$, ****$P < 0.0001$. (For interpretation of the references to colour in this figure legend, the reader is referred to the web version of this article.)

by a modest reduction on plasma TG and TC levels, no effect on atherosclerotic plaques was observed.

DHCR24 is the crucial limiting enzyme bridging the Kandutsch–Russell (K–R) pathway and the Bloch pathway of cholesterol biosynthesis, converting intermediates eventually into desmosterol. [32] In the post-lanosterol pathway, it eventually turns desmosterol into cholesterol. The vast majority of cholesterol is synthesized *de novo* by hepatocytes in the liver. Therefore, DHCR24 inhibition with SH42 leads to desmosterol accumulation in hepatocytes and excess of the desmosterol, similar to cholesterol, may be excreted as component of very low-density lipoprotein (VLDL) into the circulation. In addition, under cholesterol-free diet conditions, treatment of APOE*3-Leiden.CETP mice with SH42 leads to a modest reduction in circulating cholesterol levels. This is different from previous studies in which a cholesterol-containing diet was responsible for keeping plasma total cholesterol levels elevated. [20] Importantly, this lipid-lowering effect of SH42 treatment is completely different from the use of synthetic LXR agonists, which has been associated with hyperlipidemia, hepatic lipogenesis, and even fibrosis. [33] In contrast, SH42 did not influence hepatic neutral lipid accumulation and gene expression related to lipid lipogenesis and lipolysis in the current or any of the previous studies. [20]

Immune cells need cholesterol for activation and proliferation. Therefore we next studied the effects of DCHR24 inhibition on the immune landscape. Reassuring was that treatment with SH42 did not lead to changes in immune cell subsets in blood, spleen or bone marrow. We did, however, observe a much lower number of peritoneal cells after thioglycolate injection in mice treated with SH42. More specifically, the number of peritoneal macrophages was strongly reduced and the lavaged cells showed attenuated capacity to acquire lipids and differentiate into foam cells. It is unclear whether this effect is due to reduced recruitment or activation of monocytes, or a result of accelerated clearance of the inflammatory reagent. In a previous study we used Zymosan A as model of peritoneal cell elicitation and found enhanced clearance of the sterile infection. [18] Either way, the data combined suggest that SH42 treatment can impact immune cell function in severe inflammatory conditions, which may even be used to its advantage in the treatment of diseases of severe inflammation including sepsis. However, in more subtle, low-grade chronic inflammation, SH42 apparently has limited to no impact on the immune system.

We previously showed that SH42 treatment does not prevent atherosclerotic lesion development in hyperlipidemic female APOE*3-Leiden.CETP mice or male LDL receptor deficient mice, which we suspected to be caused by the cholesterol-containing diet provided to the mice to promote atherogenesis. Exogenous cholesterol suppresses hepatic *de novo* cholesterol synthesis, and as such also desmosterol production. In addition, excess cholesterol is known to suppress DHCR24 expression in macrophages and foam cells, to promote cholesterol efflux and slow down lesion development, [30] which would limit the efficiency of SH42. Therefore, in the current study we switched to regressive, cholesterol-free, diet, conditions also with the idea that LXR activation *via* upregulation of ABCA1/ABCG1 would mainly facilitate lesion regression rather than slowing down progression. This idea was substantiated by an early study showing that a synthetic LXR agonist facilitates atherosclerotic lesion regression in APOE*3-Leiden mice. [8] Nevertheless, we did not find accelerated lesion regression upon SH42 treatment in APOE*3-Leiden.CETP mice while switching mice from a cholesterol-containing Western-type diet to a cholesterol-free regular chow diet did lead to stabilization of the plaques. A limitation of the APOE*3-Leiden.CETP model is that only female mice develop hypercholesterolemia -in response to a cholesterol-containing Western-type diet- to an extend at which it induces atherosclerosis development. Given that previous work also demonstrated no effect of SH42 treatment on atherosclerosis development in male LDL receptor deficient mice, while it consistently did in both male and female mice in other diseases models, we believe sex not to be a critical determinant of the outcome of the current work.

To summarize, we demonstrated that treatment with DHCR24 inhibitor SH42 increases desmosterol levels in the liver and circulation, and under cholesterol-free diet conditions additionally lowers circulating cholesterol levels in APOE*3-Leiden.CETP mice. Those effects, however, did not have an impact on the immune landscape, nor did it promote atherosclerotic lesion regression.

Author Contribution

Conceptualization: J.M., L.F.Z., M.G., A.E.N., S.K., P.C.N.R.; Data curation: J.M., L.F.Z., M.H., I.S., A.E.N., S.K., P.C.N.R.; Formal analysis: J.M., L.F.Z., M.H., S.K.; Investigation: J.M., L.F.Z., J.I.V., A.E.N., M.H., S.K., P.C.N.R.; Resources: C.M., F.B., M.G., S.K., P.C.N.R.; Writing – original draft: J.M., L.F.Z., M.H.; Writing – review & editing: J.M., L.F.Z., M.P.J.W., J.I.V., A.E.N., S.K., M.H., C.M., F.B., M.G., P.C.N.R.; Supervision: M.G., S.K., M.P.J.W., A.E.N., P.C.N.R.; Funding acquisition, M.G. and P.C.N.R.

Consent to Publish declarations

Not applicable.

CRediT authorship contribution statement

Jing Miao: Writing – review & editing, Writing – original draft, Investigation, Formal analysis, Data curation, Conceptualization. **Lobke F. Zijlstra:** Writing – review & editing, Writing – original draft, Investigation, Formal analysis, Data curation, Conceptualization. **Marieke Heijink:** Writing – review & editing, Writing – original draft, Investigation, Formal analysis, Data curation. **Iulia Sidorov:** Data curation. **Jamie I. van der Vaart:** Writing – review & editing, Investigation. **Christoph Müller:** Writing – review & editing, Resources. **Franz Bracher:** Writing – review & editing, Resources. **Menno P.J. de Winther:** Writing – review & editing, Supervision. **Martin Giera:** Writing – review & editing, Supervision, Resources, Funding acquisition, Conceptualization. **Annette E. Neele:** Writing – review & editing, Supervision, Investigation, Data curation. **Patrick C.N. Rensen:** Writing – review & editing, Supervision, Resources, Investigation, Funding acquisition, Data curation, Conceptualization. **Sander Kooijman:** Writing – review & editing, Supervision, Resources, Investigation, Formal analysis, Data curation, Conceptualization.

Consent to Participate

Not applicable.

Clinical trial number

Not applicable.

Ethics

The animal experiments have been performed in compliance with the guidelines of the Dutch Act on Animal Experimentation and EU Directive 2010/63/EU, and received prior approval by the Animal Welfare Body Leiden and Central Authority for Scientific Procedures on Animals (CCD; license number AVD11600202010187).

Fundings

This work was supported by the Novo Nordisk Foundation (grant NNF18OC0032394 to M.G.), the Netherlands Cardiovascular Research Initiative CVON-GENIUS-2 (grant to M.P.J.d.W. and P.C.N.R.), the Rembrandt Institute of Cardiovascular Science (grant to S.K. and A.E.N.) and the Chinese Scholarship Council (grant 202206170032 to J.M.).

Declaration of competing interest

The authors declare that they have no known competing financial interests or personal relationships that could have appeared to influence the work reported in this paper.

Acknowledgements

We are grateful for Amanda Pronk, Reshma Lalai, Trea Streefland, Salwa Afkir (Department of Medicine, Division of Endocrinology, LUMC, Leiden, the Netherlands), and Cindy van Roomen (Department of Medical Biochemistry, Amsterdam UMC, Amsterdam, the Netherlands) for their kind technical assistance.

Appendix A. Supplementary data

Supplementary data to this article can be found online at https://doi.org/10.1016/j.steroids.2026.109830.

Data availability

The data generated during and/or analyzed during the current study are available from the corresponding author on reasonable request.

References

[1] K. Nelson, V. Fuster, M. Ridker Paul, Low-dose colchicine for secondary prevention of coronary artery disease, J. Am. Coll. Cardiol. 82 (7) (2023) 648–660.
[2] B. Wang, P. Tontonoz, Liver X receptors in lipid signalling and membrane homeostasis, Nat. Rev. Endocrinol. 14 (8) (2018) 452–463.
[3] R.K. Tangirala, E.D. Bischoff, S.B. Joseph, B.L. Wagner, R. Walczak, B.A. Laffitte, C. L. Daige, D. Thomas, R.A. Heyman, D.J. Mangelsdorf, X. Wang, A.J. Lusis, P. Tontonoz, I.G. Schulman, Identification of macrophage liver X receptors as inhibitors of atherosclerosis, Proc. Natl. Acad. Sci. USA 99 (18) (2002) 11896–11901.
[4] S.B. Joseph, E. McKilligin, L. Pei, M.A. Watson, A.R. Collins, B.A. Laffitte, M. Chen, G. Noh, J. Goodman, G.N. Hagger, J. Tran, T.K. Tippin, X. Wang, A.J. Lusis, W. A. Hsueh, R.E. Law, J.L. Collins, T.M. Willson, P. Tontonoz, Synthetic LXR ligand inhibits the development of atherosclerosis in mice, Proc. Natl. Acad. Sci. USA 99 (11) (2002) 7604–7609.
[5] X. Bi, J. Song, J. Gao, J. Zhao, M. Wang, C.A. Scipione, M.L. Koschinsky, Z. V. Wang, S. Xu, G. Fu, Activation of liver X receptor attenuates lysophosphatidylcholine-induced IL-8 expression in endothelial cells via the NF-κB pathway and SUMOylation, J. Cell. Mol. Med. 20 (12) (2016) 2249–2258.
[6] N. Terasaka, A. Hiroshima, T. Koieyama, N. Ubukata, Y. Morikawa, D. Nakai, T. Inaba, T-0901317, a synthetic liver X receptor ligand, inhibits development of atherosclerosis in LDL receptor-deficient mice, FEBS Lett. 536 (1–3) (2003) 6–11.
[7] M.N. Bradley, C. Hong, M. Chen, S.B. Joseph, D.C. Wilpitz, X. Wang, A.J. Lusis, A. Collins, W.A. Hseuh, J.L. Collins, R.K. Tangirala, P. Tontonoz, Ligand activation of LXR beta reverses atherosclerosis and cellular cholesterol overload in mice lacking LXR alpha and apoE, J. Clin. Invest. 117 (8) (2007) 2337–2346.
[8] L. Verschuren, J. de Vries-van der Weij, S. Zadelaar, R. Kleemann, T. Kooistra, LXR agonist suppresses atherosclerotic lesion growth and promotes lesion regression in apoE*3Leiden mice: time course and mechanisms, J. Lipid Res. 50 (2) (2009) 301–311.
[9] E. Vucic, C. Calcagno, S.D. Dickson, J.H. Rudd, K. Hayashi, J. Bucerius, E. Moshier, J.S. Mounessa, M. Roytman, M.J. Moon, J. Lin, S. Ramachandran, T. Tanimoto, K. Brown, M. Kotsuma, S. Tsimikas, E.A. Fisher, K. Nicolay, V. Fuster, Z.A. Fayad, Regression of inflammation in atherosclerosis by the LXR agonist R211945: a noninvasive assessment and comparison with atorvastatin, JACC Cardiovasc. Imaging 5 (8) (2012) 819–828.
[10] S.S. Im, T.F. Osborne, Liver x receptors in atherosclerosis and inflammation, Circ. Res. 108 (8) (2011) 996–1001.
[11] T.M. Yang, M. Miao, W.Q. Yu, X. Wang, F.J. Xia, Y.J. Li, S.D. Guo, Targeting macrophages in atherosclerosis using nanocarriers loaded with liver X receptor agonists: a narrow review, Front. Mol. Biosci. 10 (2023) 1147699.
[12] K. Griffett, L.A. Solt, B.E.-D.M. El-Gendy, T.M. Kamenecka, T.P. Burris, A liver-selective LXR inverse agonist that suppresses hepatic steatosis, ACS Chem. Biol. 8 (3) (2013) 559–567.
[13] K. Griffett, R.D. Welch, C.A. Flaveny, G.R. Kolar, B.A. Neuschwander-Tetri, T. P. Burris, The LXR inverse agonist SR9238 suppresses fibrosis in a model of non-alcoholic steatohepatitis, Mol Metab 4 (4) (2015) 353–357.
[14] E.D. Muse, S. Yu, C.R. Edillor, J. Tao, N.J. Spann, T.D. Troutman, J.S. Seidman, A. Henke, J.T. Roland, K.A. Ozeki, B.M. Thompson, J.G. McDonald, J. Bahadorani, S. Tsimikas, T.R. Grossman, M.S. Tremblay, C.K. Glass, Cell-specific discrimination of desmosterol and desmosterol mimetics confers selective regulation of LXR and SREBP in macrophages, Proc. Natl. Acad. Sci. USA 115 (20) (2018) E4680–E4689.
[15] X. Zhang, J.G. McDonald, B. Aryal, A. Canfran-Duque, E.L. Goldberg, E. Araldi, W. Ding, Y. Fan, B.M. Thompson, A.K. Singh, Q. Li, G. Tellides, J. Ordovas-Montanes, R. Garcia Milian, V.D. Dixit, E. Ikonen, Y. Suarez, C. Fernandez-Hernando, Desmosterol suppresses macrophage inflammasome activation and protects against vascular inflammation and atherosclerosis, Proc. Natl. Acad. Sci. USA 118 (47) (2021).
[16] C. Muller, S. Hemmers, N. Bartl, A. Plodek, A. Korner, V. Mirakaj, M. Giera, F. Bracher, New chemotype of selective and potent inhibitors of human delta 24-dehydrocholesterol reductase, Eur. J. Med. Chem. 140 (2017) 305–320.
[17] C. Muller, E. Hank, M. Giera, F. Bracher, Dehydrocholesterol reductase 24 (DHCR24): medicinal chemistry, Pharmacology and Novel Therapeutic Options, Curr Med Chem 29 (23) (2022) 4005–4025.
[18] A. Korner, E. Zhou, C. Muller, Y. Mohammed, S. Herceg, F. Bracher, P.C.N. Rensen, Y. Wang, V. Mirakaj, M. Giera, Inhibition of Delta24-dehydrocholesterol reductase activates pro-resolving lipid mediator biosynthesis and inflammation resolution, Proc. Natl. Acad. Sci. USA 116 (41) (2019) 20623–20634.
[19] E. Zhou, X. Ge, H. Nakashima, R. Li, H.J.P. van der Zande, C. Liu, Z. Li, C. Muller, F. Bracher, Y. Mohammed, J.F. de Boer, F. Kuipers, B. Guigas, C.K. Glass, P.C. N. Rensen, M. Giera, Y. Wang, Inhibition of DHCR24 activates LXRalpha to ameliorate hepatic steatosis and inflammation, EMBO Mol. Med. 15 (8) (2023) e16845.
[20] X. Ge, B. Slutter, J.M. Lambooij, E. Zhou, Z. Ying, C. Agirman, M. Heijink, A. Rimbert, B. Guigas, J. Kuiper, C. Muller, F. Bracher, M. Giera, S. Kooijman, P.C. N. Rensen, Y. Wang, M. Schonke, DHCR24 inhibitor SH42 increases desmosterol without preventing atherosclerosis development in mice, iScience 27 (6) (2024) 109830.
[21] K. Prasad, M. Mishra, Mechanism of hypercholesterolemia-induced atherosclerosis, Rev. Cardiovasc. Med. 23 (6) (2022).
[22] M. Westerterp, C.C. van der Hoogt, W. de Haan, E.H. Offerman, G.M. Dallinga-Thie, J.W. Jukema, L.M. Havekes, P.C. Rensen, Cholesteryl ester transfer protein decreases high-density lipoprotein and severely aggravates atherosclerosis in APOE*3-Leiden mice, Arterioscler. Thromb. Vasc. Biol. 26 (11) (2006) 2552–2559.
[23] R. van Eenige, P.S. Verhave, P.J. Koemans, I. Tiebosch, P.C.N. Rensen, S. Kooijman, RandoMice, a novel, user-friendly randomization tool in animal research, PLoS One 15 (8) (2020) e0237096.
[24] W. In Het Panhuis, S. Kooijman, B. Brouwers, A. Verhoeven, A.C.M. Pronk, T.C. M. Streefland, M. Giera, P. Schrauwen, P.C.N. Rensen, M. Schönke, Mild exercise does not prevent atherosclerosis in APOE*3-Leiden.CETP mice or improve lipoprotein profile of men with obesity, Obesity (Silver Spring) 28 (Suppl 1(Suppl 1)) (2020) S93–s103.
[25] E.G. Bligh, W.J. Dyer, A rapid method of total lipid extraction and purification, Can. J. Biochem. Physiol. 37 (8) (1959) 911–917.
[26] R.B. Pebriana, S. Simsek, M. Heijink, M. Giera, Rapid analysis of sterols in blood-derived samples, in: M. Giera, E. Sánchez-López (Eds.), Clinical Metabolomics: Methods and Protocols, Springer US, New York, NY, 2025, pp. 291–302.
[27] J.I. van der Vaart, R. van Eenige, P.C.N. Rensen, S. Kooijman, Atherosclerosis: an overview of mouse models and a detailed methodology to quantify lesions in the aortic root, Vascular Biology 6 (1) (2024) e230017.
[28] T. Yoshikawa, S. Hitoshi, A.-K. Michiyo, Y. Naoya, H.A. H., M. Takashi, O. Hiroaki, T. Yoshiaki, I. Yoko, O. Ken, O. Jun-Ichi, H. Kenji, G. Takanari, K. Satoshi, I. Shun, N., Yamada, Identification of liver X receptor-retinoid X receptor as an activator of the sterol regulatory element-binding protein 1c gene promoter, Mol. Cell. Biol. 21 (9) (2001) 2991–3000.
[29] A. Grefhorst, B.M. Elzinga, P.J. Voshol, T. Plosch, T. Kok, V.W. Bloks, F.H. van der Sluijs, L.M. Havekes, J.A. Romijn, H.J. Verkade, F. Kuipers, Stimulation of lipogenesis by pharmacological activation of the liver X receptor leads to production of large, triglyceride-rich very low density lipoprotein particles, J. Biol. Chem. 277 (37) (2002) 34182–34190.
[30] N.J. Spann, L.X. Garmire, J.G. McDonald, D.S. Myers, S.B. Milne, N. Shibata, D. Reichart, J.N. Fox, I. Shaked, D. Heudobler, C.R. Raetz, E.W. Wang, S.L. Kelly, M.C. Sullards, R.C. Murphy, A.H. Merrill Jr., H.A. Brown, E.A. Dennis, A.C. Li, K. Ley, S. Tsimikas, E. Fahy, S. Subramaniam, O. Quehenberger, D.W. Russell, C. K. Glass, Regulated accumulation of desmosterol integrates macrophage lipid metabolism and inflammatory responses, Cell 151 (1) (2012) 138–152.
[31] M. Hoekstra, L.M. de Jong, R. van der Geest, L.R. de Leeuw, R. Krisnamurthi, J. J. Geerling, M. Van Eck, LXR agonist T0901317's hepatic impact overrules its Atheroprotective action in macrophages, driving early Atherogenesis in chow-diet-fed male apolipoprotein E knockout mice, Biomolecules 14 (4) (2024).
[32] E.J. Zerenturk, L.J. Sharpe, E. Ikonen, A.J. Brown, Desmosterol and DHCR24: unexpected new directions for a terminal step in cholesterol synthesis, Prog. Lipid Res. 52 (4) (2013) 666–680.
[33] M. Ni, B. Zhang, J. Zhao, Q. Feng, J. Peng, Y. Hu, Y. Zhao, Biological mechanisms and related natural modulators of liver X receptor in nonalcoholic fatty liver disease, Biomed. Pharmacother. 113 (2019) 108778.